Journal of Alloys and Compounds 763 (2018) 570–580

Contents lists available at ScienceDirect

Journal of Alloys and Compounds

journal homepage: http://www.elsevier.com/locate/jalcom

Impedance spectroscopy and conduction mechanism of multiferroic $Bi_{0.8}(Ba_{0.9}Ca_{0.1})_{0.8}Fe_{0.8}(Ti_{0.9}Sn_{0.1})_{0.8}O_3$

F. Mizouri [a, *], N. Abdelmoula [a], D. Mezzane [b], H. Khemakhem [a]

[a] Laboratory of Multifunctional Materials and Applications (LaMMA), LR (16ES18), Faculty of Sciences of Sfax, University of Sfax, B.P. 1171, 3000, Sfax, Tunisia
[b] LMCN, F.S.T.G., University Cadi Ayyad, Marrakech, Morocco

ARTICLE INFO

Article history:
Received 31 March 2018
Received in revised form
24 May 2018
Accepted 25 May 2018
Available online 4 June 2018

Keywords:
Ceramic
BFO
Dielectric proprieties
Ionic conductivity

ABSTRACT

$Bi_{0.8}(Ba_{0.9}Ca_{0.1})_{0.8}Fe_{0.8}(Ti_{0.9}Sn_{0.1})_{0.8}O_3$ ceramic is synthesized by conventional solid-state reaction method and investigated by structural, Raman spectra, thermal and dielectric properties. It is crystallized in a biphasic system where it is distorted in rhombohedral-to-orthorhombic with *R3c* and *Pnma* space group, respectively. Furthermore, the ferromagnetic-paramagnetic phase transition ($T_N = 623$ K) is detected by (DSC) and Raman spectroscopy The electrical properties of this compound have been studied using complex impedance spectroscopy in the 100 Hz−100^6 MHz frequency range and temperature range 443 −703 K. During its evolution, an anomaly is observed at 623 K, which corresponds to ferromagnetic-paramagnetic transition. Two semi-circles are observed in impedance plot indicating the presence of two relaxation processes in this compound associated with the grain and grain boundary. The relaxation behavior of the grain and grain boundary of the $Bi_{0.8}$ $(Ba_{0.9}Ca_{0.1})_{0.8}$ $Fe_{0.8}(Ti_{0.9}Sn_{0.1})_{0.8}O_3$ are also obtained from the analyzed electrical modulus data. AC conductivity measured follows the power-law dependence $\sigma_{AC} \sim \omega^s$ typical for charge transport. Therefore, the experimental results are analyzed with various theoretical models. The calculated values of n_1 decreased at lower frequencies with temperature, this behavior reveals that the conduction mechanism is correlated with barrier hopping. While the observed minimum in the temperature dependence at higher frequency exponent n_2 strongly suggests that tunneling of the large polarons is the dominant transport process.

1. Introduction

In modern technology system, the multi-ferroic materials have gained strong research interest due to both the wealthy fundamental physics and the number of potential multi-functional applications with combined high piezo-electric properties. Several material systems, such as $YMnO_3$, $TbMnO_3$, $HoMnO_3$, $LuFe_2O_4$, and $BiFeO_3$ have been reported as single-phase multi-ferroic materials [1,2], the majority of which showed a multi-ferroic nature only at low temperatures. Their industrial utility is further limited by low constant magneto-electric coupling. So far, $BiFeO_3$ has been the only natural occurring material with $T_N = 643$ K and $T_C = 1143$ K possessing high intrinsic polarization (100 μC/cm^2 in the $(111)_{pc}$ direction) and offers both ferro-electric and antiferromagnetic properties above room temperature [3,4]. It has rhombohedral distorted structure with FeO_6 octahedra leading to a coupling of magnetism and ferroelectricity. Owing to its rhombohedral structure, the $BiFeO_3$ has been considered as an end-member of a variety of lead free ceramics exhibiting morphotropic phase boundary (MPB), which is believed to be the key for obtaining high piezoelectric properties suitable for high temperature applications. Moreover, the electric and magnetic properties of $BiFeO_3$ are also hampered by high dc conductivity and high coercive electric field, which arises due to the existence of multivalent Fe ions, defects and oxygen vacancies.

Kumar et *al.* [5] reported that (La,-Ti) doped $BiFeO_3$ have a lower coactivity as well as a very low value of dielectric loss (~0.03). Cheng et al. [6] studied the effect of local structural distortion on their magnetic and dielectric properties by the simultaneous substitution of $Ba^{2+}$and Ti^{4+} ions in BiFeO3 and found that doping strongly affects magnetic and dielectric properties. Deng et *al.* [7] simultaneously doped Ba and Ti into $BiFeO_3$ and found that both magnetic and ferroelectric properties of Ba doped BFO ceramics can be enhanced by Ti substitution. Its dielectric loss was reduced to 0.65 at 100 Hz, nearly one half of that of $Bi_{0.8}Ba_{0.2}FeO_3$.

In our previous work, we have studied the structure, the

* Corresponding author.
E-mail address: mizourifarhat@yahoo.fr (F. Mizouri).

https://doi.org/10.1016/j.jallcom.2018.05.353
0925-8388/

dielectric and magnetic properties of (1-x)$BiFeO_3$-x$Ba_{0.9}Ca_{0.1}$-$Ti_{0.9}Sn_{0.1}O_3$ ($0, 1 \leq x \leq 0,5$) system [8]. We have shown that the material with $x = 0.2$ presents the best magnetic properties ($M_r = 0.163$ emu/g, $H_c = 0.23$ T) at room temperature. Nevertheless, complex impedance spectroscopy is a non-destructive testing technique for analyzing the electrical processes in a compound on the application of an AC signal as input perturbation [9]. This technique is particularly useful in analyzing electrical properties of electro ceramic materials, such as relaxation characteristic, conductivity, dielectric behavior, etc. [10]. It ensures separation between the bulk, grain boundaries, and electrode electrolyte interface properties. A much more profound analysis is possible by combining the impedance analysis with use of the complex electrical formalism [11]. Then, this investigation is based on impedance characterization. The temperature transition is deduced by Raman spectroscopy.

2. Experimental

The ceramic $Bi_{0.8}(Ba_{0.9}Ca_{0.1})_{0.8}Fe_{0.8}(Ti_{0.9}Sn_{0.1})_{0.8}O_3$ is prepared using the solid state reaction method. The Bi_2O_3, Fe_2O_3, $BaCO_3$, $CaCO_3$, SnO_2 and TiO_2 powders were carefully weighed in stoichiometric proportions and thoroughly mixed in an agate mortar for 2 h. To reveal the characteristics of the synthesis of $Bi_{0.8}(Ba_{0.9}Ca_{0.1})_{0.8}Fe_{0.8}(Ti_{0.9}Sn_{0.1})_{0.8}O_3$ ceramic the stoichiometric mixture of powders corresponding to the chemical reaction in solid phase given below by the equation:

$$0.4\ Bi_2O_3 + 0.4\ Fe_2O_3 + 0.72\ BaCO_3 + 0.08\ CaCO_3 + 0.72\ TiO_2 + 0.08\ SnO_2 \rightarrow Bi_{0.8}\ (Ba_{0.9}Ca_{0.1})_{0.8}\ Fe_{0.8}\ (Ti_{0.9}Sn_{0.1})_{0.8} + 0.8\ CO_2 \uparrow$$

is thoroughly prepared.

The powders were dried and calcined at 600 °C and 700 °C for 4 h. Afterwards, the resulting mixtures were dried and pressed into 10 mm-diameter disks under 10 MPa. The disks were sintered for 4 h at an optimized temperature of 900 °C.

Crystal structure was examined via an X-ray diffraction meter with a CuKα_1 radiation (l = 1.54178 Å) XRD, D8 Advance, Bruker Inc. Modulated differential scanning calorimetry (DSC) is used to determine the transition temperature ferromagnetic to paramagnetic (T_N). Raman scattering data were collected in the 100 to 1000 cm-1 frequency range using a Raman spectrometer (HoribaHR800, Jobin Yvon). The dielectric measurements were studied using LCR meter HP 4284A in the 303–643 K and 100–100^6 Hz temperature and frequency ranges respectively.

3. Phase structure

The X-ray diffraction pattern at room temperature of the $Bi_{0.8}(Ba_{0.9}Ca_{0.1})_{0.8}Fe_{0.8}\ (Ti_{0.9}Sn_{0.1})_{0.8}O_3$ powder is illustrated in Fig. 1. The diffraction pattern of the sample consists of acute and simple diffraction peaks. The most peaks observed in the XRD correspond to $BiFeO_3$ [21], with the presence of the other peaks indicating the impurity phase of $Bi_2Fe_4O_9$ and $Bi_{25}FeO_{40}$. Indexing these peaks has been attempted in different crystal systems and unit cell configurations using a standard computer program Full prof [12]. The resulting Rietveld refinement showed that the diffracted peaks can be assigned to perovskite structures in which the rhombohedral (95.54% *R3c*) and orthorhombic (4.46% *Pnma*) phases coexist. The refinement parameters, $R_P = 10.2$, $R_{WP} = 13.8$, $R_{EXP} = 9.4$ and $\chi^2 = 2.1$, indicate a full agreement between the experimental data and the refinement model used in the analysis. In fact, they show the selected diffracted region of the main XRD peaks (around 32°), confirming the applicability of the structural model employed in the structural refinement (*R3c* and *Pnma*). This procedure resulted

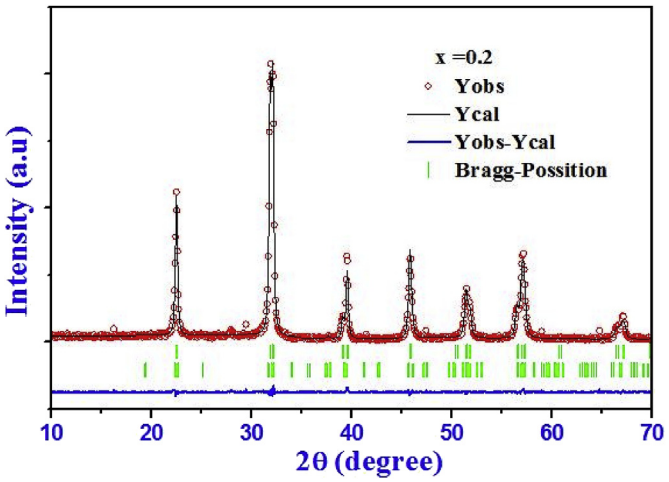

Fig. 1. XRD pattern for $Bi_{0.8}\ (Ba_{0.9}Ca_{0.1})_{0.8}\ Fe_{0.8}\ (Ti_{0.9}Sn_{0.1})_{0.8}O_3$ at room temperature.

in lattice parameters and structural angles consistent with a structural model composed of *R3c* and *Pnma* phases (*R3c*: unit cell: $a = b = 5.5832$, $c = 13.8642$, $\alpha = \beta = 90$ and $\delta = 120$; and *Pnma*, orthorhombic unit cell: $a = 5.6191$, $b = 5.6623$, $c = 4.0112$, $\alpha = \delta = 90$, and $\beta = 90.48$).

4. Calorimetric study

Fig. 2 shows the subtracted DSC measurement background of the BFO sample. In fact a clear peak due to ferromagnetic to paramagnetic transition is seen in the spectrum. The Neel temperature (T_N) obtained (~623 K) matches well the reported value of BFO [3,4].

5. Temperature evolution of the Raman spectra

Raman spectroscopy is said to be a very useful technique in the study of the transitionals characteristics phases and the local structure modulations in the electric materials [13]. Now, we discuss the evolution of the Raman signature around the ferromagnetic–paramagnetic (FM–PM) transition phase ($T = 623$ K). We performed a Raman spectroscopy experiment to

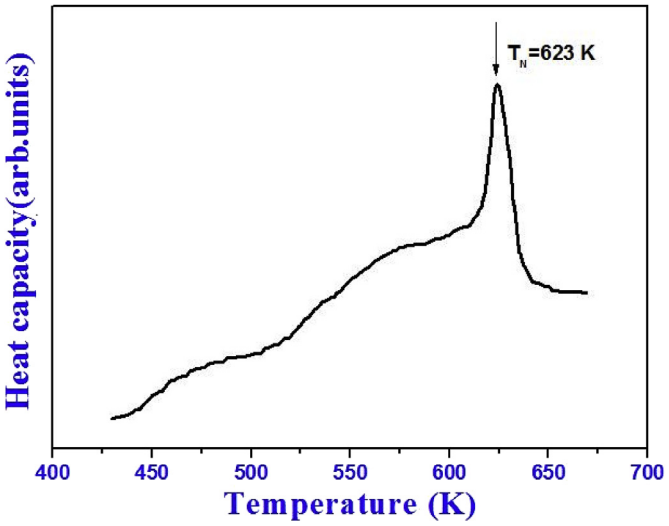

Fig. 2. DSC curve $Bi_{0.8}\ (Ba_{0.9}Ca_{0.1})_{0.8}\ Fe_{0.8}\ (Ti_{0.9}Sn_{0.1})_{0.8}O_3$ sample shows the ferromagnetic–paramagnetic transition (T_N).